Impact Factor (SJIF): 6.092 E-ISSN: 2583-1615

International Journal of Research in Academic World

Received: 02/February/2023 IJRAW: 2023; 2(3):168-174 Accepted: 14/March/2023

Influence of Processing on the Structural and Transport Properties of PLZT Systems

[*1]Vijendra A Chaudhari

[*1]Department of Physics, Dayanand Science College, Latur, Maharashtra, India.

Abstract

Polycrystalline samples of the solid-solution series $(Pb_{1-x}La_x)(Zr_{1-y}Ti_y)_{1-0.25x}O_3$, for x = 0.02, 0.04, 0.06, 0.08, and 0.10, were synthesized using the solid-state reaction technique. Structural, morphological, and dielectric characterization studies were performed for all the samples. Structural phase analysis was carried out using X-ray powder diffraction. All samples in the solid-solution series (PLZT) exhibited a rhombohedral single phase in the concentration range $0.02 \leq x \leq 0.06$, whereas the samples with x = 0.08 and 0.10 showed a cubic phase. Microstructural studies for all the samples were conducted using SEM. The SEM analysis revealed nearly uniform grain distribution, indicating a uniform microstructure with no abnormal grain growth.

Dielectric studies—dielectric constant (ε) and tangent loss (tan δ)—measured as a function of temperature (from room temperature (RT) to 900 K) at different frequencies showed that the compounds undergo a diffuse-type ferroelectric–paraelectric phase transition. Diffusivity analysis of the phase transition yielded values between 1 and 2, indicating variation in the degree of disorder within the system.

Keywords: PLZT ceramics, Diffuse Phase Transition, Relaxor Ferroelectrics, X-ray Diffraction, Dielectric Characterization.

Introduction

Amongst the many ferroelectrics, some oxides with perovskite structure of general formula ABO_3, (A = mono- or divalent, B = tri-hexavalent ions) are in the forefront both in the area of research as well as in industrial applications. La- and Zr-doped lead titanate (PLT, PLZT) powder ceramics and thin films are known to have interesting dielectric, pyroelectric, electrooptic and piezoelectric properties [1–4], and so have a wide range of applications such as infrared sensors [5], capacitors [6], ferroelectric memories (dynamic random access memory (DRAM) and nonvolatile random access memory (NVRAM)) [7], shutters [2], optical modulators [8], etc.

Ferroelectric lead zirconate titanate $Pb(Zr_{1-x}Ti_x)O_3$ (PZT) powders are known to exhibit high piezoelectric and pyroelectric properties [9–11]. These materials are also known for their unusual phase boundary, called the morphotropic phase boundary (MPB) [12], which occurs at around 50% Zr substitution for Ti in $PbTiO_3$, and which separates two structural phases: rhombohedral (Zr-rich region) and tetragonal (Ti-rich region) structures; in particular, a very high piezoelectric response is recorded in the MPB. The occurrence of the MPB depends mainly on the procedure of preparation of the samples and the grain sizes [13, 14].

Substitution of lanthanum for lead (PLZT) in these materials changes their macroscopic properties from normal ferroelectric to relaxor ferroelectric types; the relaxation phenomenon affects deeply PLZT properties (anomalies). In particular, high values of dielectric permittivity and electromechanical and electrooptic coefficients are recorded, which make these materials suitable for various applications such as capacitors, optoelectronic modulators, etc. [15–17]. These anomalies manifest themselves within a broad temperature region around a temperature, T_m, corresponding to the maximum in the dielectric permittivity; the phase transition is called 'diffuse phase transition' (DPT). Several models and approaches have been developed to interpret this DPT involving different mechanisms: chemical heterogeneities, superparaelectric behaving due to mesoscopic heterogeneities etc. [18–22]. As mentioned above, a maximum response of different characteristics, among them the electromechanical coupling coefficient, is obtained due to the coexistence of ferroelectric tetragonal and ferroelectric rhombohedral phases near the MPB.

In view of the above we have synthesized and studied structural phase evolution, morphology, DSC, electrical and dielectric properties as a function of temperature (33 – 560 ^{0}C) and frequency (5 Hz to 13MHz). In this paper we report the effect of La substitution on the structural and dielectric properties of PLZT samples.

Experimental

Commercially available high purity ingredient oxides: $PbCO_3$ (99.9% purity; Aldrich chemicals), La_2O_3 (99.9% purity; Aldrich chemicals), ZrO_2 (99.9% purity; Aldrich chemicals)

***Corresponding Author:** Vijendra A Chaudhari

and TiO_2 (99.9% purity; Loba chemie.) were used as the starting materials. The polycrystalline samples of $(Pb_{1-x}La_x)(Zr_{1-y}Ti_y)_{1-0.25x}O_3$ (PLT) (x = 0.02, 0.04, 0.06, 0.08 and 0.1) were synthesized by a high-temperature conventional mix oxide method under air atmosphere. To prevent PbO loss or vaporization during the high-temperature sintering, 5% by weight excess of PbO was added. The excess PbO helps to compensate for the lead evaporation during sintering process. The constituent compounds in a suitable stoichiometry were thoroughly mixed and wet ground using an agate mortar and pestle for 2 hr. The sieved fine powders were then calcined in an alumina crucible at temperature ranging from 450-550 ^{0}C for 8 hr. in air atmosphere and brought to room temperature under slow cooling. The process of grinding was repeated and the ground material was sieved through 75μm (200 mesh). The sieved fine powder was cold pressed into cylindrical pallets of size 10 mm and 1-2 mm of thickness using hydraulic press at a pressure of 50 MPa. The pellets were sintered in an air atmosphere at 900 ^{0}C for 12 hr. The formation and quality of the compound were checked by an X-ray diffraction (XRD) technique. Densities of the sintered pellets were measured by Archimedes principle. Porosity was evaluated from the observed and theoretical densities (X-ray). The grain morphology and average grain size were determined using SEM. The average grain size was determined by using a linear intercept method. The average particle size was determined from the full width at half maximum using Scherrer's equation [80].

The X-ray diffraction of the compounds was recorded at room temperature using X-ray powder diffractometer (Xpert Pro-PAN Philips) with Cu K□ radiation (λ = 1.5418 A) in a wide range of Bragg angles 2θ ($10^0 \leq 2\theta \leq 80^0$) with a scanning rate of 0.02^0/min. The surface morphology of the pellets was studied by scanning electron microscopy (SEM) (JEOL JSM-6360 A). The dielectric measurements were obtained on electroded-sintered pellets with air-drying silver paste and dried at 150^{0}C for 2 hr. Measurements were made isothermally allowing thermal equilibrium by leaving the furnace at the preset temperature for 30 min on these disk samples and the data were recorded using computer-controlled HP 4192A LF HEWLETT PACKARD impedance analyzer over a wide range of temperature (33 – 560^{0}C) and frequency (5Hz – 13MHz) with an applied voltage of 1.3 V.

Results and Discussion

Fig. 1 (a) shows the room temperature x-ray diffraction pattern of $PbTiO_3$. On the basis of the agreement between the d-observed and calculated values, it has been confirmed that the compound belong to the tetragonal system with the lattice parameters a = 3.9023 A and c = 4.0657 A. The X-ray analysis showed that at room temperature for X ≤ 6 samples of 65/35 PLZT are rhombohedral. Within this composition range the distortion angle, 90-□ and the lattice constant decreases as X increases. For samples with X = 8 and 10 the X-ray data showed the presence of Bragg's peaks corresponding to cubic phase. Figs. 1 (b, c, d, e, f) show the room temperature X-ray diffraction patterns of all the samples of the $(Pb_{1-x}La_x)(Zr_{1-y}Ti_y)_{1-0.25x}O_3$ (PLZT) for X/65/35 = 2, 4, 6, 8, and 10 series respectively. The room temperature X-ray powder diffraction data has been analyzed to identify the structure of the phases present in each sample. All the XRD patterns exhibit the presence of sharp Bragg peaks suggesting the formation of single compounds. All the Bragg peaks were indexed and lattice parameters were determined using a standard computer program package. The analysis of X-ray results show that there is a systematic change in the observed structural phase as the La content is increased. The experimental density was measured using Archimedes principle. The fraction of porosity has been evaluated from:

$$\frac{\rho_b}{\rho_{th}} = 1 - f_p$$

Where f_p is the fraction of porosity and ρ_{th} is the theoretical density obtained from X-ray results and % porosity was calculated for the samples. The fraction of theoretical density could be expressed as:

$$f_p = \frac{\rho_{th} - \rho_b}{\rho_{th}}$$

The fraction of theoretical density (%), porosity, lattice parameters and the unit cell volume for all the composition of the PLZT series are tabulated in Table 1**.** The results show that density decreases with increasing La content. Fig. 2 shows the variation of fraction of theoretical density as a function of La content.

Grain size of the PLZT samples estimated from SEM samples and particle size estimated from XRD as a function of Lanthanum concentration are shown in Fig. 3. Fig 4 (a) – (e) illustrate microstructure of the PLZT samples sintered at 900^{0}C. The micrograph shows a dense material consisting of relatively uniform grains. The size of the grain increases with the increment of La content. It is consistent with the results of other authors [23]. Under air atmosphere sintering condition, high temperature leads to some volatilization of PbO formed more A-site vacancies and less B-site vacancies distributed in the lattice of PLZT X/65/35. Based on it, the A-site vacancies and amount of lanthanum impurity make a great influence on the microstructure evolutions in the system. The mechanism of the microstructure evolutions of PLZT X/65/35 ceramics with the La content variation can be understood as follows:

For the La content from 2 to 10 mol%, during the sintering of samples, the impurities of La^{3+} ions follow the grain boundary diffusion, and the A-site vacancies follow the vacancy diffusion. Because the size of La^{3+} ionic radius is vary close to the size of Pb^{2+} ionic radius, the La^{3+} ions have the preferential to inhabit the A-site vacancies, while creating much cationic vacancies in the microstructure of PLZT. As a result, the A-site La^{3+} ions and the cationic vacancies make a influence on constant of the crystal lattice. When the A-site La^{3+} ions content is more than 6% it leads to rhombohedral to cubic structure and the rhombohedral phase has been gradually transferred to cubic phase.

The characteristic temperature dependence of the dielectric content for the sample X/65/35 for x = 6 is shown in Figs. 5. The general trend seems to indicate a relaxor–ferroelectric type behavior. From the nature of the graph it is seen that the value of ε' increases gradually with rise in temperature and reached to a maximum value ε'_{max} at a particular temperature known as Curie temperature (T_c). It is also observed that the dielectric maximum (ε'_{max}) at T_c decreases with increasing frequency. The value of ε'_{max} is larger at lower frequency (0.1 kHz). Another interesting feature that is observed the value of T_c shifts towards the higher temperature side with increase in frequency, the dielectric dispersion is absent at high temperatures beyond T_c whereas the dielectric constant has been observed to decrease with increasing frequencies at temperature around and lower than T_c. This indicates strong dielectric dispersion at temperatures around and below T_c. The T_c value shifts from 430-535 K for X = 6, with the increased

frequency value 0.1 kHz to 1000 kHz. As a temperature rises, the thermally activated flips of Polar Regions and their interaction in the material lead to a gradual increase in the permittivity of the system. The appearance of dielectric peak may be attributed to phase transition (ferroelectric – paraelectric) in the material. On further rise in temperature, there is a rapid loss of the polarization in the material. This result in the monotonous fall of dielectric constant with rise in temperature beyond T_c [24, 25]. It is also seen that the dielectric constant is higher at the lower frequency.

Figs. 6 show the temperature dependence of dissipation factor at various frequencies for composition X/65/35 were X = 6. From these plots it can be seen that the values of tanδ are invariant with the rise of temperature nearly 500 k for 0.1 kHz and 1 kHz. For higher frequency (100 kHz and 1000 kHz) the values of dissipation factor nearly remain constant up to 700K. Above 500k and 700K the dissipation factor begins to increase with a rise of temperature. At higher temperatures it can be seen that the rate of increase of tanδ is higher for lower frequencies. The degree of disorder or diffuseness (i.e. diffusivity) γ in the phase transition of PLZT was calculated using the equation [26] $(1/\varepsilon - 1/\varepsilon_{max}) \alpha (T - T_c)^{\gamma}$ where ε is the dielectric constant at temperature T and ε_{max} is its maximum value at T_{max}. The value of γ calculated from graphs (Fig 7) was found within a range $1.06 < \gamma < 1.79$. This confirms that diffuse phase transition occurs in the materials with a high degree of disorder. The value of γ was found to increase as a function of X. The deviation of the phase transition behavior from the Curie-Weiss type can thus be interpreted as the existence of disordering [27] in this system. The variation of Curie temperature with composition, dielectric data and diffusivity γ are listed in Table 2.

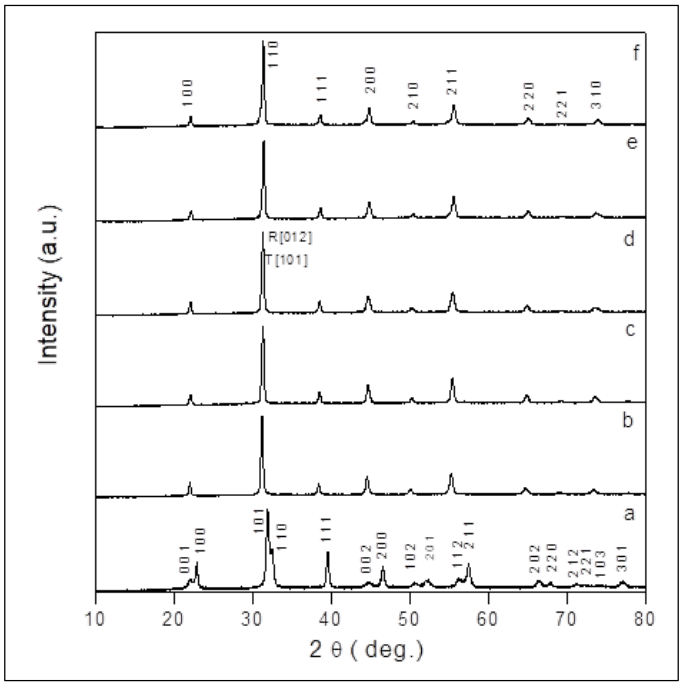

Fig 1: Room temperature X-ray diffraction patterns of $(Pb_{1-x}La_x)(Zr_{1-y}Ti_y)_{1-0.25x}$ $(2 \leq x \leq 10)$. (a = 0, b = 2, c = 4, d = 6, e = 8, f = 10)

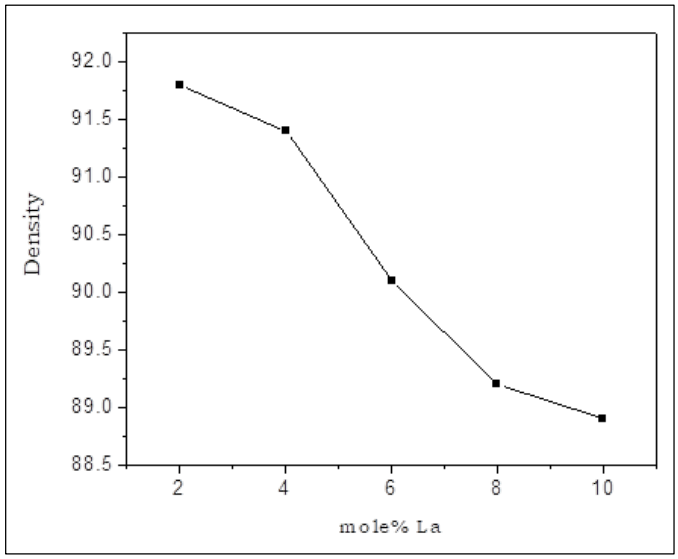

Fig 2: Variation of density of PLZT as a function of mol%La content $(2 \leq x \leq 10)$

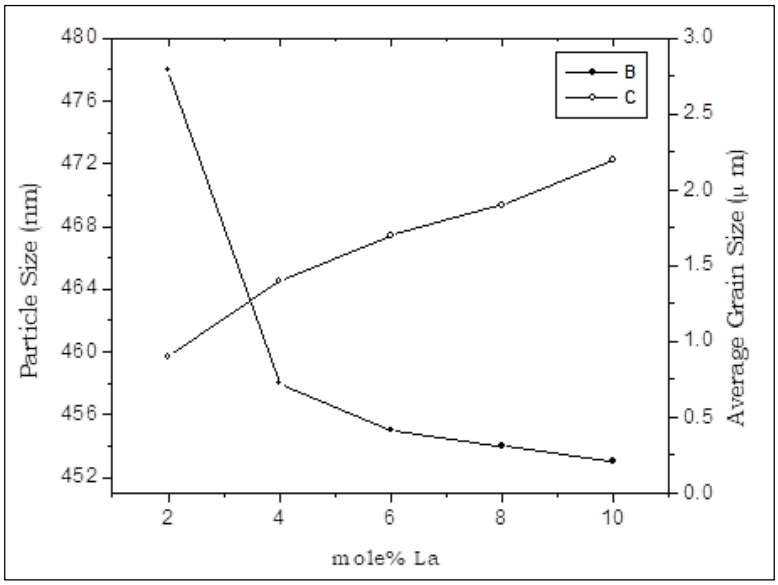

Fig 3: Variation of particle size and grain size as a function of mole% La content ($2 \leq x \leq 10$).

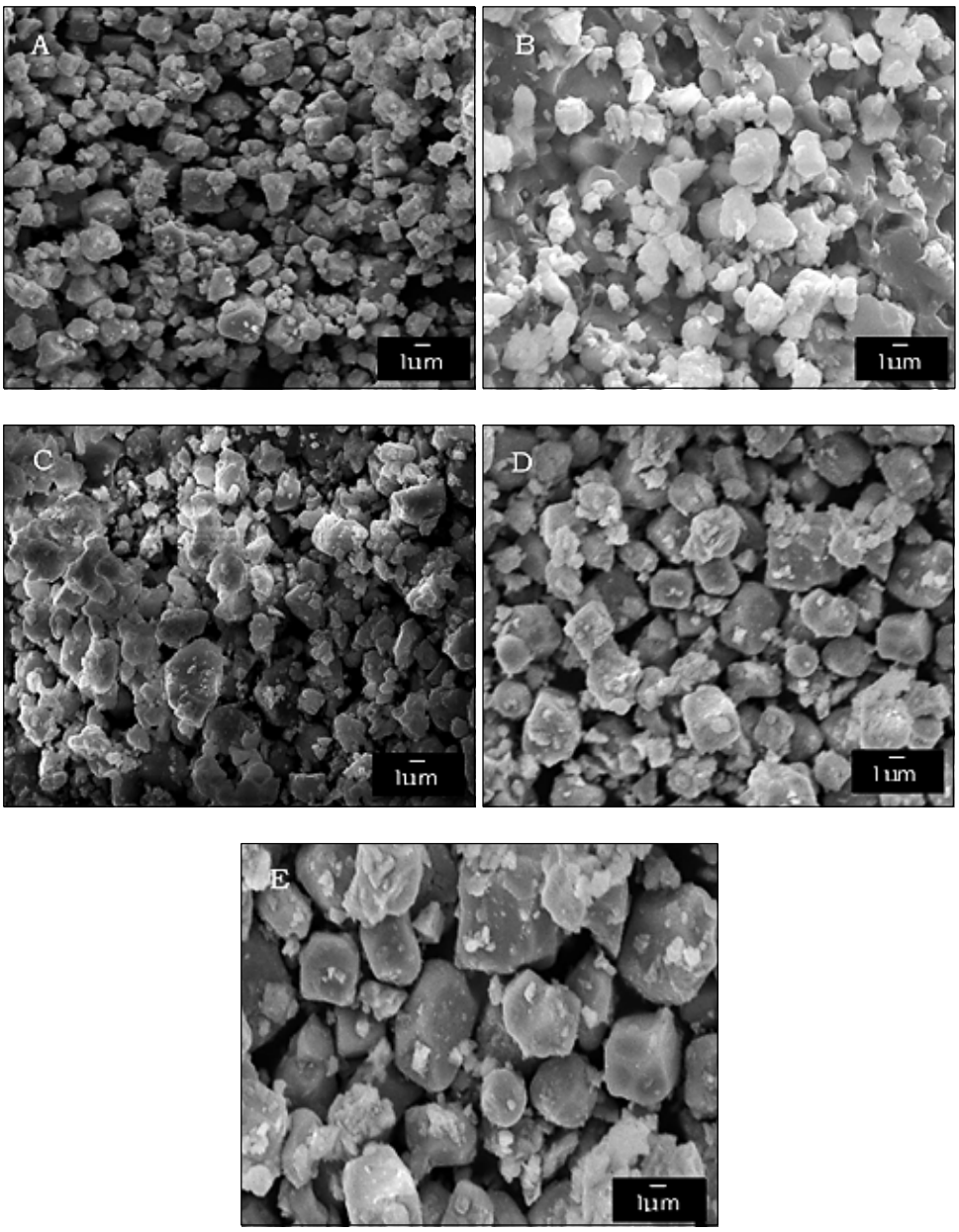

Fig 4: SEM micrographs of $(Pb_{1-x}La_x)(Zr_{1-y}Ti_y)_{1-0.25x}$ at (A) x = 2, (B) x = 4, (C) x = 6, (D) x = 8 and (E) x = 10

Table 1: Lattice parameters of PLZT ceramics of $(Pb_{1-x}La_x)(Zr_{1-y}Ti_y)_{1-0.25x}O_3$.

Composition (X)	Lattice parameter a_R	Phase & Space Group	α (deg)	Unit Cell Volume V ($\AA^3$)	Fraction of Theoretical Density (%)	Porosity (%)
2/65/35	4.0916	R3m	89.94	68.50	91.8	8.1
4/65/35	4.0839	R3m	89.96	68.11	91.4	8.5
6/65/35	4.0824	R3m	89.97	68.03	90.1	9.2
	a_C					
8/65/35	4.0725	Pm3m	90.00	67.54	89.2	9.6
10/65/35	4.0704	Pm3m	90.00	67.44	88.9	10

(a_R = Rhombohedral Phase, a_C = Cubic phase)

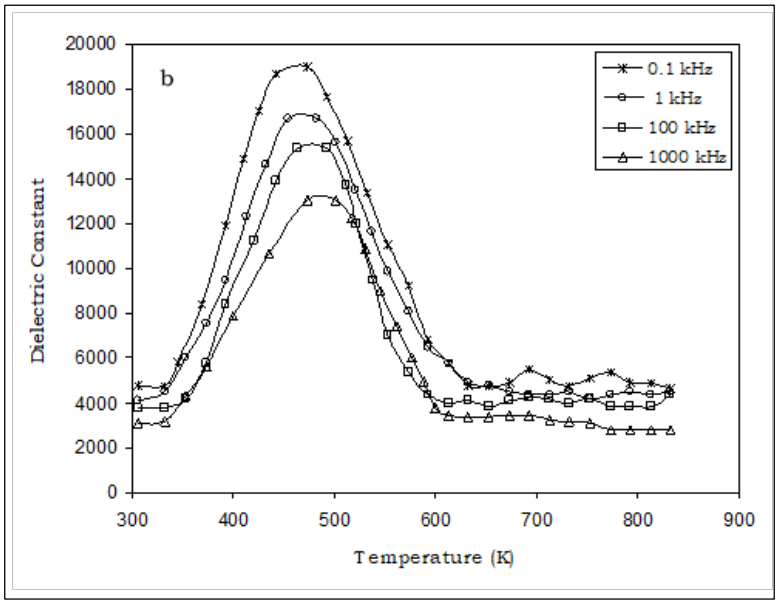

Fig 5: Temperature dependence of Dielectric Constant of $(Pb_{1-x}La_x)(Zr_{1-y}Ti_y)_{1-0.25x}$ at different frequencies for x = 6.

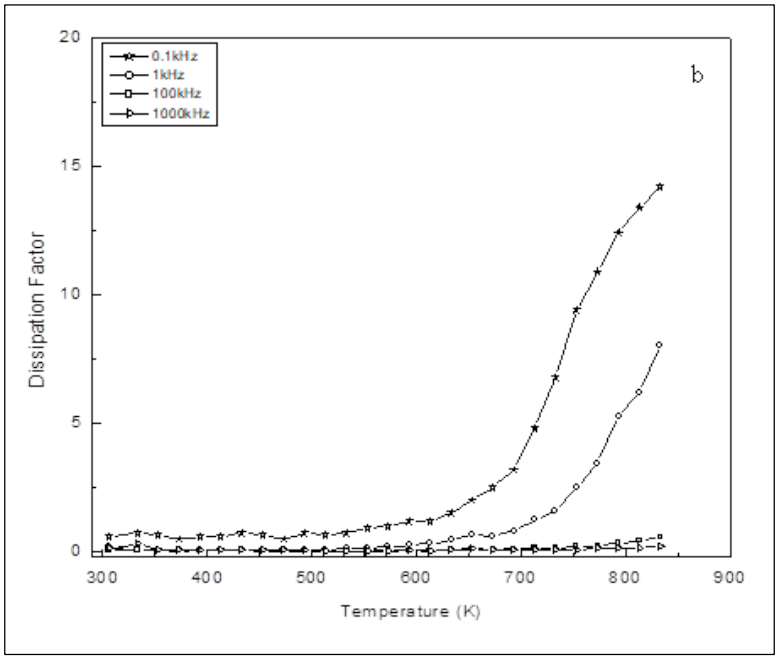

Fig 6: Temperature dependence of Dissipation factor of $(Pb_{1-x}La_x)(Zr_{1-y}Ti_y)_{1-0.25x}$ at different frequencies for x = 6.

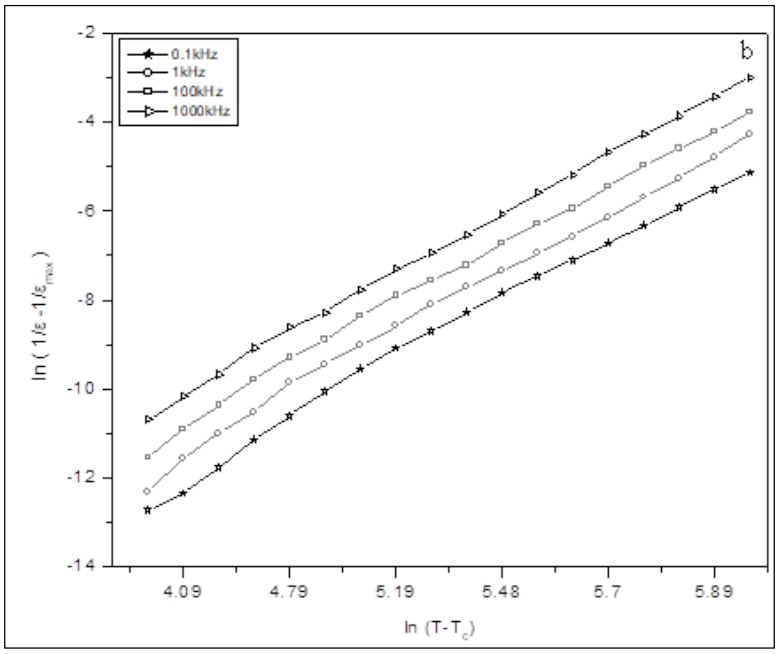

Fig 7: Plots of ln $(1/\varepsilon - 1/\varepsilon_{max})$ vs. ln$(T-T_c)$ of $(Pb_{1-x}La_x)$ $(Zr_{1-y}Ti_y)_{1-0.25x}$ Ceramics at different frequencies for x = 6.

Table 2: Dielectric parameters of $(Pb_{1-x}La_x)$ $(Zr_{1-y}Ti_y)_{1-0.25x}$. ceramics for x = 2, 6 and 10 for different frequencies.

Composition (x) (La)	Frequency (kHz)	εRT	tanδRT	Tmax (°C)	εmax	tanδ at Tmax	γ
2/65/35	0.1	6105	0.42	312	26403	3.79	1.12
	1	5708	0.09	325	24609	1.03	1.06
	100	5400	0.07	334	22300	0.10	1.07
	1000	5215	0.05	341	19611	0.07	1.08
6/65/35	0.1	5753	0.59	168	18650	0.67	1.78
	1	4120	0.19	182	1630	0.29	1.79
	100	3751	0.13	195	15340	0.17	1.77
	1000	3149	0.09	205	13210	0.08	1.76
10/65/35	0.1	4023	0.28	55	7203	0.25	1.44
	1	3771	0.19	63	5624	0.21	1.42
	100	3128	0.11	71	5259	0.15	1.46
	1000	2201	0.07	79	4405	0.08	1.57

Conclusion

PLZT ceramics have been prepared using the high-temperature conventional mix oxide method and their structural, microstructural and dielectric properties were studied. XRD revealed the existence of the MPB phase ($X \leq 6$), and that addition of lanthanum tends to transform the average symmetry of the sample to a cubic one. Lattice parameters, unit cell volume, theoretical density and porosity were found to vary with La content. The morphological studies using SEM showed nearly uniform grain distribution i.e. uniform microstructure with no abnormal grain growth. Dielectric properties change from those of normal ferroelectrics to those of relaxors ferroelectrics, with relatively low temperatures of the dielectric constant, with increasing La content, as shown by dielectric measurements. The dielectric studies provide many interesting features of the materials, such as the shift in transition temperature, diffuse phase transition and modification of dielectric properties.

References

1. Haertling GH, Land CE. Hot-pressed (Pb,La)(Zr,Ti)O3 ferroelectric ceramics for optical memory and display devices. *J Am Ceram Soc*. 1971; 54(1):1-11.
2. Land CE, Thacher PP. Ferroelectric ceramic electro-optic materials and devices. Proc IEEE. 1969; 57(5):751-768.
3. Wright JS, Francis LF. Phase-development in Si-substituted PZT thin-films. *J Mater Res*. 1993; 8(7):1712-1720.
4. Haertling GH. Lanthanum-doped lead zirconate titanate (PLZT) ceramics: PZT revisited. *J Am Ceram Soc*. 1999; 82(4):797–818.
5. Iijima K, Tomita Y, Takayama R, Ueda I. Preparation of c-axis oriented PbTiO3 thin films and their crystallographic, dielectric, and pyroelectric properties. *J Appl Phys*. 1986; 60(1):361-367.
6. Bersani D, Lottici PP, Montenero A, Pigoni S. Raman spectra of sol-gel derived lead titanate. *J Mater Sci*. 1996; 31(12):3153–3157.
7. Lee SJ, Kang KY, Han SK, Jang MS, Chae BG, Yang YS, *et al*. Raman scattering of (Pb,La)TiO3 thin films. Appl Phys Lett. 1998; 72(3):299–300.
8. Ishida M, Matsunami H, Tanaka T. Preparation of ad-oriented PbTiO3 ferroelectric thin films by RF sputtering. Appl Phys Lett. 1977; 31(7):433-434.
9. Scott JF, Araujo CA. Ferroelectric memories. Science. 1989; 246(4936):1400-1405.

10. Larsen PK, Cuppens R, Spierings GACM. Ferroelectric and dielectric properties of thin PZT films for 4 Mbit ferroelectric nonvolatile memories. Ferroelectrics. 1992; 128(1):265-270.
11. Evans JT, Womack R. An experimental 512-bit nonvolatile memory with ferroelectric storage cell. *IEEE J Solid-State Circuits*. 1988; 23(5):1171-1175.
12. Jaffe B, Cook WR, Jaffe H. Piezoelectric Ceramics. London: Academic Press; 1971.
13. Kakegawa K, Matsunaga O, Kato T, Sasaki Y. Compositional modification of PLZT ceramics by a new wet-chemical method. *J Am Ceram Soc*. 1995; 78(4):1071-1075.
14. Meng JF, Katiyar RS, Zou GT, Wang XH. Raman scattering in Pb1−xLaxTiO3 ceramics. Phys Status Solidi A. 1997; 164(2):851-862.
15. Smolenskii GA, Bokov VA, Isupov VA, Krainik NN, Pasynkov RE, Sokolov AI. Ferroelectrics and Related Materials. New York: Gordon and Breach; 1984. p. 763.
16. Ramesh R, editor. Thin Film Ferroelectric Materials and Devices. Boston: Kluwer Academic Publishers; 1997.
17. Haertling GH. PLZT electrooptic materials. In: Buchanan RC, editor. Ceramic Materials for Electronics. New York: Marcel Dekker; 1986. p. 139.
18. Kirillov VV, Isupov VA. Relaxation polarization of PbMg1/3Nb2/3O3 (PMN). A ferroelectric with a diffused phase transition. Ferroelectrics. 1973; 5(1):3-9.
19. Burns G, Dacol FH. Crystalline ferroelectrics with glassy polarization behavior. *Phys Rev B*. 1983; 28(5):2527-2530.
20. Cross LE. Relaxor ferroelectrics. Ferroelectrics. 1987; 76(1):241-267.
21. Li S, Eastman JA, Newnham RE, Cross LE. Susceptibility of nanometer-sized ferroelectric particles. *Phys Rev B*. 1997; 55(18):12067-12071.
22. Viehland D, Li JF, Jang SJ, Cross LE, Wuttig M. Glassy polarization in the ferroelectric Pb(Mg1/3Nb2/3)O3. *Phys Rev B*. 1991; 43(10):8316-8320.
23. Zhang Y, Ding AL, Qiu PS, He XY, Zheng XS, Zheng HR, *et al*. Dielectric properties of La-doped PZT ceramics. Mater Sci Eng B. 2003; 99(1-3):360-363.
24. Cheng ZY, Katiyar RS, *et al*. Dielectric relaxation in the Pb1−xLax(Zr0.65Ti0.35)1−x/4O3 relaxor ferroelectric system. Phys Rev B. 1998; 57(14):8166-8177.
25. Yao X, Chen ZL, Cross LE. Polarization and depolarization behavior of hot pressed lead lanthanum zirconate titanate ceramics. *J Appl Phys*. 1983; 54(6):3399-3403.
26. Pilgrim SM, Sutherland AE, Winzer SR. Dielectric properties of the Pb(Mg1/3Nb2/3)O3-PbTiO3-BaTiO3 system. *J Am Ceram Soc*. 1990; 73(10):3122-3125.
27. Stenger CGF, Burggraaf AI. Order-disorder reactions in the ferroelectric perovskite Pb(Sc1/2Nb1/2)O3. *J Phys Chem Solids*. 1980; 41(1):25-30.